

Supporting Information (SI)

Theoretical Analysis on transient photon-generated voltage in polymer based organic devices.

5

To further confirm the conclusion in the manuscript, a theoretical model, simultaneously taking into account the possible excitons and carrier processes in the active polymer layer after photo excitation and the interaction of different polar species formed in different phases has been developed. The interphasic and intraphasic interactions have to be considered in the studies of Device No.1, 2 and 3. For Device No.2 and Device No.3, since one pristine polymer is used for these devices, intraphasic interaction will dominate the processes. However, as polymer blend is used in Device 1, both interphasic and intraphasic interactions will exist. The details are discussed as follows.

15

We present a time-dependent device model, describing the dynamical processes of both excitons induced by light illumination and charge carriers created from the exciton dissociation in pristine polymer layer and blend layer. Then we calculate the transient photovoltage (TPV) in single-layer organic photovoltaic cells. With the model, the theoretical TPV has been determined and analyzed with the experimental results for further verifying the conclusion of this work.

Considering (1) the laser pulse transmits into the polymer layer through the ITO side; (2) the absorption length of polymer layer is much less than the thickness of polymer layer in our devices, for example, for Device No. 3, the absorption length is around 100 nm and thickness of P3HT layer is around 240nm and (3) the exciton lifetime is ultra-short with a value around 500 ps, excitons will have very little population near interface of polymer layer/Al which will thus be ignored in the model. Consequently, the photon-to-carrier conversion near the buried interface of ITO/polymer layer dominates the TPV. Fig. S1 shows the six main processes of (i)-(vi) in the photon-to-carrier conversion near the buried interface.

30

Fig. S1 describes the basic photo-to-carrier conversion processes in pristine polymer layer based device. (i), (ii), (iii), (iv), (v) and (vi) denote exciton dissociation in the active layer, drift current, diffusion current, thermionic current, interface recombination, and dissociation current in the buried interface, respectively. (ii) Drift current is the electric current, or movement of charge carriers, which is due to the applied electric field describing the electromotive force over a given distance. (iii) Diffusion current is a current in a semiconductor caused by diffusion of charge carriers (holes and/or electrons). Diffusion current can be in the same or opposite direction of a drift current. (iv) Thermionic current is the heat-induced flow of charge carriers across an interface with a potential-energy barrier. This occurs because the thermal energy given to the carrier overcomes the energy barrier between the metal and polymer layer. As for (i),(v) and (vi), the photogenerated excitons near the buried interface can undergo either recombination (v) or direct dissociation to the free carriers in the active layer (i) through some intraphasic interactions, such as exciton-carrier interaction, and captured by the anode (vi) respectively. Theoretically, several methods have been studied in the static system. Similar to its inorganic counterpart, Onsager's theory was applied to organic systems to solve the relation between dissociation rate of exciton and electric field.^{1,2} Meanwhile, a so-called device model method has also been applied to simulate the physical process in different organic devices.^{2,3} But those steady-state methods cannot describe the transient results of TPV experiments. Therefore, a time-dependent method is necessary to be developed appropriately for our work.

The *first* issue is the dynamics of excitons generated by the laser pulse. The diffusion equation is as follows:

$$\frac{\partial}{\partial t} \rho_{ex}(x,t) = D \frac{\partial^2}{\partial x^2} \rho_{ex}(x,t) + G(x,t) - \frac{\rho_{ex}(x,t)}{\tau} \quad (1)$$

where ρ_{ex} is the density of excitons, D the diffusion coefficient, τ the lifetime of excitons, $x=0$ is at buried interface (ITO/polymer) and $x=L$ at top interface (i.e. L is the thickness of polymer layer). The generation function $G(x, t)$ follows the form of the input laser pulse, i.e. $G(x, t) = g_0 \exp(-x/L_a)$ when $t \geq t_{off}$ or $t \leq t_{on}$ and $G(x, t) = 0$ where g_0 is the generation rate of excitons depending on the light intensity. L_a is the absorption length, and t_{on} ($=0$) and t_{off} are the time when the laser is on and off, respectively. All these parameters are determined by experiments.

As mentioned above, L_a is less than L , while the diffusion length of exciton is commonly less than 10 nm. The exciton dissociation mainly happens in a small region near the buried interface of ITO/polymer layer. We thus have the analytic solution of Eq. (1) as feature of excitons.

$$5 \quad \rho_{ex}(x, t) = \rho_{ex}^{(0)} \xi(t) e^{(-x/L_a - t/\tau_{eff})} \quad (2)$$

where $\rho_{ex}^{(0)} = g_0 \tau_{eff} (e^{-t_{on}/\tau_{eff}} - 1)$, $\xi(t) = (e^{t/\tau_{eff}} - 1) / (e^{t_{off}/\tau_{eff}} - 1)$

for $0 < t < t_{off}$ and $\xi = 1$ for $t > t_{off}$, and the effective lifetime of excitons $\tau_{eff} \equiv (1/\tau - D/L_a^2)^{-1}$ which represents an important feature of excitons.

The second issue is the dynamics of charge carriers. The time-dependent continuity equations, with a drift-diffusion current density, coupled to the Poisson's equation are given as,

$$10 \quad \frac{\partial \rho_{n(p)}}{\partial t} = -J_{n(p)} + G_{ca} - R \quad (3)$$

where $\rho_{n(p)}$ is the electron(hole) density, $J_{n(p)}$ the current density, G_{ca} the carrier generation rate, and R the recombination rate in the materials.

$$15 \quad J_{n(p)} = -\mu_{n(p)} \left[\pm E \rho_{n(p)} + \frac{kT}{e} \frac{\partial \rho_{n(p)}}{\partial x} \right] \quad (4)$$

$$\frac{\partial \rho_{n(p)}}{\partial x} = \frac{e}{\varepsilon_0 \varepsilon} (\rho_p - \rho_n) \quad (5)$$

e is the magnitude of the electron charge, so that the total electric current density $J \equiv e(J_p - J_n)$; $\mu_{n(p)}$ is the mobility, E the electric field, kT is set to room temperature, the sign takes $+(-)$ for electron (hole), and the Einstein's relation has been used;⁴ ε_0 is the static dielectric constant, and ε is the relative permittivity, which will be set to be 3.0. Eqs.(3)–(5) can be solved numerically with appropriated boundary conditions³. For example, the current for holes at the buried interface ($x=0$) is,

$$J_p(0) = AT^2 \left[e^{(-\phi + eV)/kT} - \rho_p(0) / \rho_0 \right] \quad (6)$$

where A is Richardson's constant, ϕ is the injection barrier from electrode to organic material, ρ_0 the maximum density of electrons and holes which are set to be 1.0 nm^{-3} for both carriers, and V the potential induced by space charge, which is given as

$$V = E_0(t)r_c / 4 \quad (7)$$

where $E_0(t)$ is the strength of electric field at the corresponding interface and the capture radius $r_c = e^2 / (4\pi\epsilon_0\epsilon kT)$, which denotes the region in which the Coulombic binding energy of the image charge in the electrode to the carriers is larger than kT . The expressions for electrons are similar. The different types of currents considered in this work are shown in Fig. S1.

We then combine the two parts above. The carrier generation is from the excitation of the laser pulse, that is, $G_{ca} = G_{ex}$, where G_{ex} is the generation of excitons and μ is the corresponding dissociation rate in the process (i) in Fig. S1.⁵ Meanwhile, G_{ex} is proportional to the carrier density at the buried interface $\rho_{ex}(0,t)$. So we have the generation of charge carriers due to the exciton dissociation $G_{ca} = \Gamma_0 \xi(t) e^{(-t/\tau_{eff})}$, where the strength Γ_0 is proportional to the intensity of the input laser pulse and μ has been included in Γ_0 .

As the final step, we show the calculation of photovoltage. The commonly used form of open-circuit voltage in static state is invalid here, because the interfacial effect and influence of space charge are largely neglected in the derivation and the generated carrier can hardly maintain in the bulk in the transient measurement (i.e. no open-circuit voltage is obtained).⁶ For TPV, however, the generated charge carriers, by the dissociation of excitons, concentrated mainly in a small region at the interface, cause an extra electric field. The electric field will make a voltage drop (which can be an instantly large voltage change) in the organic material side of the buried interface. Accordingly the Fermi energy at the electrodes is changed, so the TPV signal should be well approximated the voltage change and give the information of time-dependent Fermi energy change of the buried interface, that is, $\Delta V = V(t) - V(t=0)$, where $V(t)$ is the time evolution of the potential in Eq. (7).

In the following, we show our main theoretical and experimental results. We first take Device No.3 as the example since the negative TPV is observed for the first time. Its structure is ITO/P3HT (230 nm)/Al.

The wavelength of the pulsed laser beam is 355 nm. The absorption length is about 100 nm, the pulse energy is 0.2 mJ, and the pulse width is 0.8 ns. The work function of bared ITO and Al is 4.7 eV and 4.3 eV respectively, and LUMO and HOMO of P3HT is 3.2 eV and 5.1 eV respectively. The effective lifetime of excitons τ_{eff} is taken to be 0.5 ns.

By studying the theoretical TPV of ITO/P3HT/Al shown in Fig. S2 (which is in good agreement with the experimental one), μ_n and μ_p are extracted as $2 \times 10^{-4} \text{ cm}^2/\text{Vs}$ and $4 \times 10^{-4} \text{ cm}^2/\text{Vs}$ respectively. Besides, the dipole formation is inferred to be 0.5 eV which is high enough to shift the work function of ITO to become slightly lower than Al, which further confirms the conclusion in the main text about the origin of negative TPV of Device No. 3. This is the key factor to cause the negative TPV.

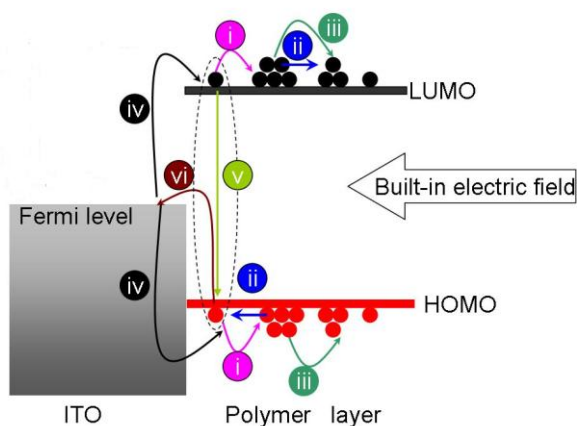
To further explain the experimental polarity change in TPV of ITO/P3HT:PCBM/Al in Fig. S2, we use the current density expressions (4) and (6). When the pulse laser is switched on, electrons generated by exciton dissociation accumulate at the buried interface and cause a large signal at the beginning. The excitons in P3HT and PCBM move to the boundary between two phases. The strong interphasic interaction makes the charge transfer occur in the Donor (P3HT)-Acceptor (PCBM) system as schematically shown in Fig. S3. For the excitons formed in Donor (P3HT), the electrons are consequently transferred to the LUMO of the Acceptor, while, for the excitons formed in Acceptor (PCBM), the holes are transferred to the HOMO of Donor. The generated electrons and holes in charge transfer state can be easily dissociated to free carriers in the separated phases of PCBM and P3HT respectively. Since the dissociation efficiency at the donor-acceptor interface is much higher than other two dissociation ways, namely, buried interfacial dissociation (step (vi) in Fig. S1) and the bulk dissociation (step (i) in Fig. S1),⁷ the electrons and holes transport in the separated channels, which is fully consistent with the results of section 2.1 “Biphasic feature of TPV in Device No.1”. However, the biphasic TPV in Fig. S2 is not the simply superimposing of two separated TPV in two channels. Because in the calculation, we found that the interphasic Columbic interaction, such as the carrier-carrier interaction or carrier-exciton interaction in blends exist simultaneously and thus the carrier mobility in each separated phase is lower than that in the pristine polymer layer. Therefore, the simulated electron and hole mobilities are expected to be $< 2 \times 10^{-2} \text{ cm}^2/\text{Vs}$ (which is μ_n of the pure PCBM in Fig. S2) and $< 4 \times 10^{-4} \text{ cm}^2/\text{Vs}$ (which is μ_p of the pure P3HT). In this theoretical calculation, the μ_n and μ_p are estimated to be $4 \times 10^{-3} \text{ cm}^2/\text{Vs}$ and $1.5 \times 10^{-4} \text{ cm}^2/\text{Vs}$ which are within the expected range.

If we neglect the interphasic interaction, the bi-exponential fitting used in the main text can be regarded as a simplified method, which can reflect the mobility balance qualitatively. Therefore, in our theory finding, the polarity change is indeed caused by

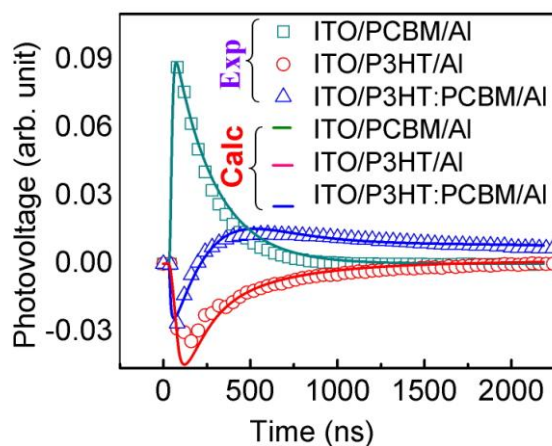
the electrons transporting in PCBM, which is the origin of positive component in biphasic TPV in Fig. S2, and the holes transporting in P3HT leading to the negative component. Since the charge transfer occurs between P3HT phase and PCBM phase in the bulk layer, we regard the polarity change as a bulk effect. Noticeably, there is another buried interface effect which can also cause the polarity change in our theoretical prediction: in a short period of time, the drift and diffusion currents increase quickly especially for electrons which describe the transport of electrons inside PCBM, inducing a field which cancels the influence of dissociation current and changes the polarity of photovoltage. However, this process is much faster than the bulk effect, which is calculated to be in the order of <20ns. However, the turning point of biphasic TPV in this work is in the time scale of 250ns. Consequently, the bulk effect dominates the polarity change in the TPV of Device No.1. This completes the description of the polarity change in TPV. In our recent study, we also find that the biphasic TPV in ITO/P3HT/Al near the turn-on point at 10ns as shown in Fig. S4. The finding proves the prediction of our theory about the existence of buried interface effect, and will be discussed in details in the subsequent literature. Here, the results of Fig. S4 can further confirm that our model is scientific sound after considering all the possible photo-physical processes.

Reference

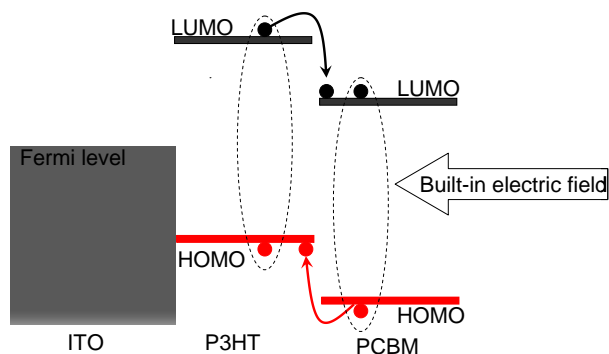
1. O. Rubel, S. D. Baranovskii, W. Stolz, and F. Gebhard, *Phys. Rev. Lett.* 100, 196602 (2008).
2. L. J. A. Koster, E. C. P. Smits, V. D. Mihailetschi, and P. W. M. Blom, *Phys. Rev. B* 72, 085205 (2005).
3. P. S. Davids, I. H. Campbell, and D. L. Smith, *J. Appl. Phys.* 82, 6319(1997).
4. The Einstein's relation should be more complicate in disordered organic materials, see, e.g., Y. Rocihman and N. Tessler, *Appl. Phys. Lett.* 80, 1948 (2002). (However, in the TPV measurements, disorder is not significant and the conventional form is still valid.).
5. M. D. Tabak and P. J. Warter, *Phys. Rev.* 173, 899 (1968)
6. C. M. Ramsdale, J. A. Barker, A. C. Arias, J. D. MacKenzie, R. H. Friend and N. C. Greenham, *J. Appl. Phys.* 92, 4266 (2002).
7. S. H. Park, A. Roy, S. Beaupre, S. Cho, N. Coates, J. S. Moon, D. Moses, M. Leclerc, K. Lee and A. J. Heeger, *Nat. Photon.* 3, 297 (2009)
8. G. Li, V. Shrotriya, J. S. Huang, Y. Yao, T. Moriarty, K. Emery and Y. Yang, *Nat. Mater.* 4, 864 (2005).



5 Fig. S1. The schematic view of currents for electron and hole at the buried interface in the pristine polymer based active layer . Fermi surface of ITO and LUMO and HOMO of polymer are represented. Arrows (i), (ii), (iii), (iv), (v) and (vi) denote dissociation of exciton in active layer, drift current, diffusion current, thermionic current, interface recombination, and dissociation current, respectively. The dash ellipse bounded an electron and a hole denotes an exciton.



10 Fig. S2 Theoretical calculation and experimental results of ITO/P3HT/AI, ITO/PCBM/AI and ITO/P3HT:PCBM/AI



7 Fig. S3 The schematic view of charge transfer occurring in the blended polymer layer. The dash ellipse bounded an electron and a hole denotes an exciton.

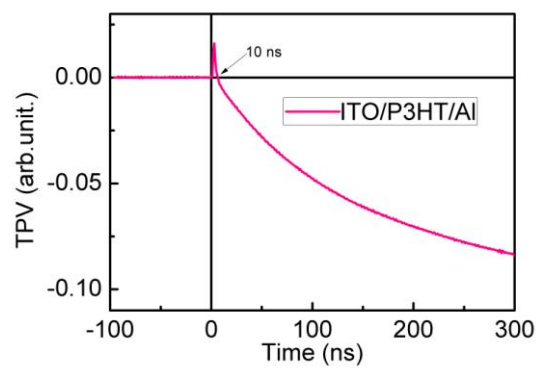


Fig. S4. Amplifying range of TPV near the turn-on point.